Chapter 3

Partitioned Element Methods

This chapter defines a general class of polytopal element formulations referred to as partitioned element methods (PEM). The essential characteristics and mathematical requirements placed upon these methods are formally stated, giving rise to a family of different approaches, for which some formal investigations are conducted in subsequent chapters. Several specific formulations are summarized in detail, and a number of existing methods are herein classified as particular instances of partitioned element methods.

3.1 Overview

Partitioned element methods are finite element-like methods which approach the task of constructing shape functions on arbitrary polytopal element domains by partitioning each element into sub-domains (quadrature cells). The element partition serves a dual purpose: it is used to establish a composite quadrature rule for the element, and to define a finite dimensional function space, from which the element's shape functions are selected as the solutions to corresponding boundary value problems, defined locally on the element.

Partitioned element methods are motivated by the idea that it is generally easier and more efficient to define complicated functions over arbitrary domains if the functions are defined in a piecewise polynomial fashion over simpler sub-domains. This is precisely the mentality which likewise motivates the finite element method and other related numerical approximation methods.

The PEM is driven by the need for establishing stable and efficient quadrature rules

on arbitrary polytopes. Unlike virtual element methods which typically circumvent the use of quadrature altogether, partitioned element methods recognize the necessity of using domain quadrature rules to evaluate nonlinear residual and stiffness contributions. The use of sufficient quadrature also yields a stable integration of the weak form which does not rely upon unphysical stabilization parameters.

In contrast with traditional perspectives which regard the shape functions as being continuously defined on element domains (i.e. generalized barycentric coordinates), the PEM exploits the fact that the shape functions and their gradients only need to be evaluated at a discrete number of quadrature points. With this in mind, PEM approximation spaces are deliberately constructed around the quadrature cell partition of the element, and consequently resemble finite element approximation spaces.

The resulting shape functions on each element are altogether subject to the conditions of approximability, compatibility, stability, and quadrature consistency, as discussed in chapter 2. Together, these conditions impose a number of unique requirements upon the element's partition, it's corresponding quadrature rules, and the associated cell-based approximation spaces.

In the following sections, an abstract framework for the PEM is established, describing the shape function boundary value problems defined on an element, and their corresponding approximations. We further enumerate several specific partitioned element methods, and provide an assessment of their potential strengths and weaknesses.

3.2 Definition of Element Shape Functions

Consider the structure of a polyhedral element $\Omega \subset \mathbb{R}^3$, as depicted in Figure 3.1. The element's boundary $\partial\Omega$ may be subdivided into a set of polygonal faces $\mathcal{T}_F(\Omega) = \{F_i\}_{i=1}^{N_F}$, such that each face F_i is shared entirely with an adjacent element, or with the mesh boundary. Corresponding sets of linear edges $\mathcal{T}_E(\Omega) = \{E_i\}_{i=1}^{N_E}$ and nodes $\mathcal{T}_V(\Omega) = \{V_i\}_{i=1}^{N_V}$ result by considering the sets of all unique intersections $\mathcal{T}_E(\Omega) = \{\partial F_i \cap \partial F_j \neq \emptyset \ \forall i \neq j\}$ and $\mathcal{T}_V(\Omega) = \{\partial E_i \cap \partial E_j \neq \emptyset \ \forall i \neq j\}$, respectively.

The function spaces to which the element's shape functions belong are effectively

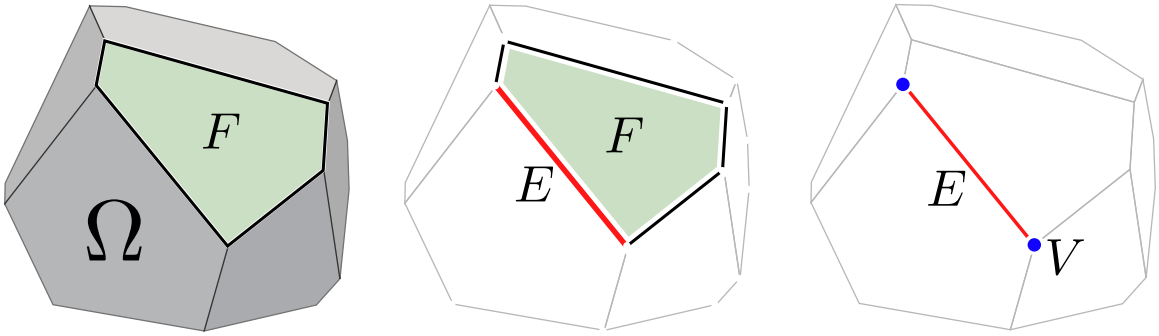

Figure 3.1. A representative polyhedral element $\Omega \subset \mathbb{R}^3$, and it's corresponding sets of faces, edges, and nodes.

broken Sobolev spaces, where a given shape function $\varphi \in \mathcal{W}_k(\overline{\Omega})$ is defined independently on the open interior of each polyhedral element $\Omega \subset \mathbb{R}^3$, and on its boundary $\partial\Omega$, such that

$$\mathcal{W}_k(\overline{\Omega}) = \left\{ \varphi|_\Omega \in H^k(\Omega) : \mathcal{L}_\Omega \varphi = f_\Omega \text{ in } \Omega,\ \varphi|_F \in \mathcal{W}_k(\overline{F})\ \forall F \in \partial\Omega \right\}, \tag{3.1}$$

$$\mathcal{W}_k(\overline{F}) = \left\{ \varphi|_F \in H^k(F) : \mathcal{L}_F \varphi = f_F \text{ in } F,\ \varphi|_E \in \mathcal{W}_k(\overline{E})\ \forall E \in \partial F \right\}, \tag{3.2}$$

$$\mathcal{W}_k(\overline{E}) = \left\{ \varphi|_E \in H^k(E) : \mathcal{L}_E \varphi = f_E \text{ in } E,\ \varphi|_V \in \mathbb{R}\ \forall V \in \partial E \right\}. \tag{3.3}$$

In essence, a given function $\varphi|_\Omega \in H^k(\Omega)$ defined on the element's interior is related to a corresponding boundary function $\varphi|_{\partial\Omega} = \bar{\varphi}$ (which itself is a broken $H^k(\partial\Omega)$ function) via a well-posed Dirichlet boundary value problem:

$$\mathcal{L}_\Omega \varphi = f_\Omega \quad \forall \mathbf{X} \in \Omega \quad \text{s.t.} \quad \varphi = \bar{\varphi} \quad \forall \mathbf{X} \in \partial\Omega, \tag{3.4}$$

where $\mathcal{L}_\Omega$ denotes a linear differential operator, and $f_\Omega \in L^2(\Omega)$ is a generic forcing function. The element's degrees of freedom are collectively accounted for in the boundary function $\bar{\varphi}$ and the forcing function f_Ω. Consequently, the interior function $\varphi|_\Omega$ is uniquely defined, provided there exists a unique solution to (3.4). In turn, we suppose that $\varphi|_F \in H^k(F)$ is the solution to a similar (2-dimensional) boundary value problem defined on each face F, and $\varphi|_E \in H^k(E)$ is the solution to a (1-dimensional) BVP on each edge E.

The advantage of defining shape functions in this manner is that it affords a great deal of flexibility in the construction of arbitrary order interpolants (or enhancement functions), while maintaining $C^0(\mathcal{B}_0)$ continuity at inter-element interfaces. Moreover,

given that the shape functions are uniquely defined at every point $\mathbf{X} \in \Omega$, they are amenable to post-processing and visualization-related tasks.

Harmonic Shape Functions

The simplest choice of $\mathcal{L}_\Omega = -\nabla^2$ and $f_\Omega = 0$ corresponds to Laplace's equation:

$$\nabla^2 \varphi = 0 \quad \forall \mathbf{X} \in \Omega \quad \text{s.t.} \quad \varphi = \bar{\varphi} \quad \forall \mathbf{X} \in \partial\Omega, \tag{3.5}$$

whose solution φ is harmonic on Ω (and likewise on each face F and edge E – refer to Figure 3.2). Harmonic shape functions form a partition of unity, are linearly complete, and arise from degrees of freedom $\varphi|_V$ borne only by the nodes of each element; therefore, they satisfy the kronecker delta property. As such, harmonic shape functions are classifiable under the category of generalized barycentric coordinates.

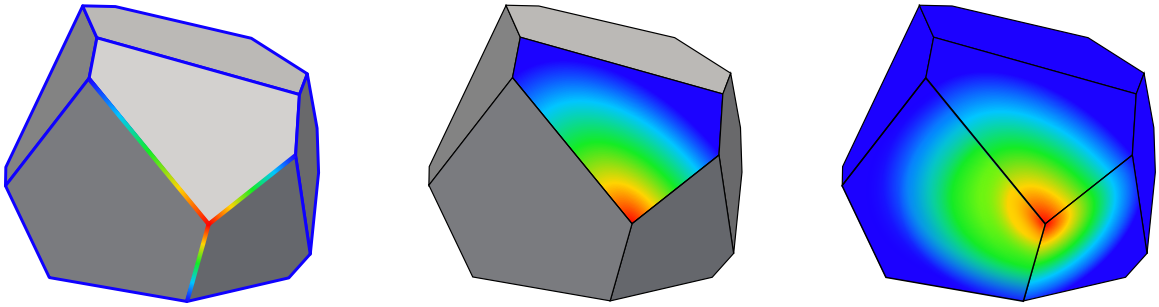

Figure 3.2. The harmonic shape function corresponding to a given node, defined hierarchially on each edge, face, and the element.

If instead $f_\Omega \neq 0$ (corresponding to Poisson's equation), then

$$-\nabla^2 \varphi = f_\Omega \quad \forall \mathbf{X} \in \Omega \quad \text{s.t.} \quad \varphi = \bar{\varphi} \quad \forall \mathbf{X} \in \partial\Omega, \tag{3.6}$$

and we may introduce additional degrees of freedom through f_Ω belonging to edges, faces, or element domains. These degrees of freedom are not necessarily associated with nodal evaluations of φ, but instead may be designed to exhibit certain desirable characteristics (to recover a particular order of polynomial completeness). The solution φ to (3.6) is not harmonic; instead, we shall refer to functions which satisfy (3.6) as *generalized harmonic shape functions*.

Harmonic shape functions are not a new concept; Gordon and Wixom were among the first authors to propose the idea in [22], and Martin et al. later considered their

application to polyhedral finite elements in [30]. However, obtaining exact solutions to (3.5) is generally infeasible for arbitrary polyhedra. In practice, approximate solutions must be considered.

In particular, Bishop has proposed a method for constructing FE approximations to harmonic shape functions in [4]. Additionally, the VETFEM ([36], [38]) and the original PEM presented in [37], may be viewed as techniques for obtaining discrete approximations to harmonic shape functions. Likewise, many virtual element methods ([7], [11], [12]) suppose that the element shape functions are harmonic over individual element domains, though they are never explicitly constructed or represented as such.

It herein becomes of interest to determine suitable approximations to harmonic shape functions on arbitrary polyhedra. A number of methods to achieve this end are subsequently discussed.

3.3 Shape Function Approximation Methods

The exact solution $\varphi \in \mathcal{U}(\Omega) = \{\varphi \in H^1(\Omega) : \varphi = \bar{\varphi}\, \forall \mathbf{X} \in \partial\Omega\}$ to (the more general) Poisson's equation in (3.6) also satisfies the equivalent weak form:

$$\int_\Omega (\nabla^2 \varphi + f_\Omega)\eta \, dV = 0 \quad \forall \eta \in \mathcal{U}_0(\Omega), \tag{3.7}$$

or

$$\int_\Omega \nabla\varphi \cdot \nabla\eta \, dV - \int_{\partial\Omega} \frac{\partial\varphi}{\partial N}\eta \, dA = \int_\Omega f_\Omega \, \eta \, dV \quad \forall \eta \in \mathcal{U}_0(\Omega), \tag{3.8}$$

where $\mathcal{U}_0(\Omega) = \{\eta \in H^1(\Omega) : \eta = 0\, \forall \mathbf{X} \in \partial\Omega\}$ denotes an appropriately defined space of admissible variations – test functions.

A vast array of different variational methods may be employed to obtain an approximate solution $\varphi^h \in \mathcal{U}^h(\Omega)$ satisfying

$$\int_\Omega \nabla\varphi^h \cdot \nabla\eta^h \, dV - \int_{\partial\Omega} \frac{\partial\varphi^h}{\partial N}\eta^h \, dA = \int_\Omega f_\Omega \, \eta^h \, dV \quad \forall \eta^h \in \mathcal{U}_0^h(\Omega), \tag{3.9}$$

where $\mathcal{U}^h(\Omega)$ and $\mathcal{U}_0^h(\Omega)$ are taken to be finite-dimensional approximation spaces. Consequently, it is of interest to determine the essential requirements placed upon a given approximation φ^h for the purposes of evaluating weak form integrals.

Specifically, for a finite element approximation to the model problem given in (2.36), consider the evaluation of an element's local bilinear form $a_\Omega(\mathbf{u}, \mathbf{v})$, where $\mathbf{u} = \sum_{a=1}^{N} \varphi_a \mathbf{u}_a$ and $\mathbf{v} = \sum_{a=1}^{N} \varphi_a \mathbf{v}_a$ are written in terms of the element's shape functions $\{\varphi_a\}_{a=1}^{N}$. An approximate evaluation of $a_\Omega(\mathbf{u}, \mathbf{v})$ is obtained by making the substitution $a_\Omega(\mathbf{u}^h, \mathbf{v}^h)$, where $\mathbf{u}^h = \sum_{a=1}^{N} \varphi_a^h \mathbf{u}_a$ and $\mathbf{v}^h = \sum_{a=1}^{N} \varphi_a^h \mathbf{v}_a$ are instead represented in terms of the approximations $\left\{\varphi_a^h\right\}_{a=1}^{N}$ to the element's shape functions.

According to the virtual element decomposition proposed in [11], we may express a given function $\mathbf{u} = \Pi_k^\Omega \mathbf{u} + (\mathbf{u} - \Pi_k^\Omega \mathbf{u})$ in terms of a low-order polynomial part $(\Pi_k^\Omega \mathbf{u})$ (up to degree k) and a non-polynomial part $(\mathbf{u} - \Pi_k^\Omega \mathbf{u})$, where $\Pi_k^\Omega : L^2(\Omega) \mapsto P^k(\Omega)$ is a corresponding polynomial projection operator satisfying $a_\Omega(\Pi_k^\Omega \mathbf{u}, \mathbf{v} - \Pi_k^\Omega \mathbf{v}) = 0 \ \forall \mathbf{u}, \mathbf{v}$, and thus

$$a_\Omega(\mathbf{u}, \mathbf{v}) = a_\Omega(\Pi_k^\Omega \mathbf{u}, \Pi_k^\Omega \mathbf{v}) + a_\Omega(\mathbf{u} - \Pi_k^\Omega \mathbf{u}, \mathbf{v} - \Pi_k^\Omega \mathbf{v}). \tag{3.10}$$

The first term appearing in the right-hand side of (3.10) accounts for the consistency of the finite element approximation, whereas the second term provides stability. To maintain consistency, the first term must be computed exactly, to the extent that

$$a_\Omega(\Pi_k^\Omega \mathbf{u}, \Pi_k^\Omega \mathbf{v}) = a_\Omega(\Pi_k^\Omega \mathbf{u}^h, \Pi_k^\Omega \mathbf{v}^h), \tag{3.11}$$

yielding the $k-$consistency property:

$$a_\Omega(\Pi_k^\Omega \mathbf{u}^h, \mathbf{v}^h) = a_\Omega(\Pi_k^\Omega \mathbf{u}, \mathbf{v}) \quad \forall \mathbf{v} \in \mathcal{V}^h(\Omega). \tag{3.12}$$

However, the second term need only be sufficiently well-approximated by

$$a_\Omega(\mathbf{u} - \Pi_k^\Omega \mathbf{u}, \mathbf{v} - \Pi_k^\Omega \mathbf{v}) \approx a_\Omega(\mathbf{u}^h - \Pi_k^\Omega \mathbf{u}^h, \mathbf{v}^h - \Pi_k^\Omega \mathbf{v}^h), \tag{3.13}$$

to the extent that the correct order of convergence is maintained, and the inf-sup condition is altogether satisfied. In [11], this is characterized by the assertion that there exist two positive constants a_* and a^* which are independent of the chosen discretization, such that the following stability condition holds:

$$a_* a_\Omega(\mathbf{v}, \mathbf{v}) \leq a_\Omega(\mathbf{v}^h, \mathbf{v}^h) \leq a^* a_\Omega(\mathbf{v}, \mathbf{v}) \quad \forall \mathbf{v} \in \mathcal{V}^h(\Omega). \tag{3.14}$$

It is argued that these conditions are necessary and sufficient to guarantee convergence of the resulting method when the local approximations $\mathbf{u}^h$ and $\mathbf{v}^h$ are used in place of $\mathbf{u}$ and $\mathbf{v}$.

It should be remarked that the evaluation of $a_\Omega(\mathbf{u}, \mathbf{v})$ will be further approximated through the use of numerical quadrature on Ω, denoted as $a^h_\Omega(\mathbf{u}, \mathbf{v})$. Incidentally, the use of low-order quadrature rules may alternatively be viewed as an exact integration of corresponding low-order approximations to $\mathbf{u}$ and $\mathbf{v}$, i.e. $a^h_\Omega(\mathbf{u}, \mathbf{v}) = a_\Omega(\mathbf{u}^h, \mathbf{v}^h)$, and is therefore subject to the conditions previously described.

With the above considerations borne in mind, we propose a set of requirements on the approximation space $\mathcal{U}^h(\Omega)$ (and $\mathcal{U}^h_0(\Omega)$):

(I) $\Pi^\Omega_k \varphi = \Pi^\Omega_k \varphi^h \ \forall \varphi \in \mathcal{U}(\Omega)$, and therefore $\mathcal{U}^h(\Omega) \supset P^k(\Omega)$.

(II) The approximation method used to obtain φ^h should yield $\lim_{N\to\infty} ||\varphi^h - \varphi||_\Omega = 0$ as the dimension N of $\mathcal{U}^h(\Omega)$ (and $\mathcal{U}^h_0(\Omega)$) is systematically increased.

Continuous Galerkin Approximations to Generalized Harmonic Shape Functions

Consider finite dimensional sub-spaces $\mathcal{U}^h(\Omega) \subset \mathcal{U}(\Omega)$ and $\mathcal{U}^h_0(\Omega) \subset \mathcal{U}_0(\Omega)$. The Galerkin approximation $\varphi^h \in \mathcal{U}^h(\Omega)$ to a given (generalized) harmonic shape function $\varphi \in \mathcal{U}(\Omega)$ satisfies

$$\int_\Omega \nabla\varphi^h \cdot \nabla\eta^h \, dV = \int_\Omega f_\Omega \, \eta^h \, dV \quad \forall \eta^h \in \mathcal{U}^h_0(\Omega). \tag{3.15}$$

Bishop has already explored such an approach for constructing approximations to harmonic shape functions using an FE discretization of a given polyheral element into sub-dividing tetrahedra. The corresponding shape function approximations $\varphi^h \subset C^0(\Omega)$ are obtained as the solutions to a set of local finite element problems defined on Ω (and its faces, edges – refer to Figure 3.3). Moreover, it was demonstrated in [4] that the resulting approximations preserve low-order polynomial completeness – a consequence of $\mathcal{U}^h(\Omega) \supset P^1(\Omega)$. If the elements are discretized into a sufficient number of tetrahedra, the method is observed to be both stable and consistent (provided a gradient correction scheme is employed to account for the effects of integration error).

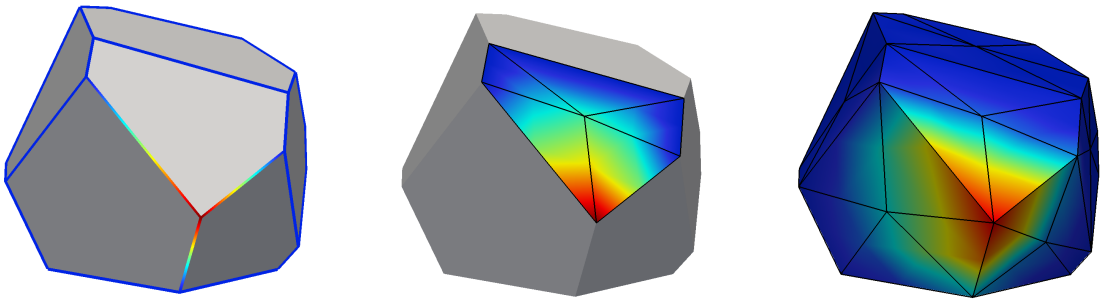

Figure 3.3. The finite element approximation to a given harmonic shape function, defined hierarchially on each edge, face, and the element.

This approach can become computationally expensive if the elements are subdivided into an excessively large number of tetrahedra, in the event that more accurate approximations to the shape functions are desired. However, initial numerical investigations have suggested that relatively coarse tetrahedral sub-divisions of the elements provide sufficiently accurate results; further subdivision (tetrahedral $h-$refinement) does little to improve the overall accuracy of the approach.

A natural extension of the method proposed by Bishop to higher-order serendipity elements would be to consider $p-$refinement of an element's tetrahedral subdivision to recover higher-order polynomial completeness, i.e. to guarantee $\mathcal{U}^h(\Omega) \supset P^k(\Omega)$ for some desired polynomial order k. Unfortunately, the construction of shape functions on a given element would likely bear a much higher computational cost with increasing polynomial degree. The specification of stable and accurate numerical quadratures would present an additional challenge.

Yet another generalization would be to consider subdividing the elements into arbitrary polyhedra, and solving (3.15) by means of the virtual element method. This would allow for a more natural collocation of quadrature cells with the specified subdivision, akin to the partitioned element method proposed in [37].

However, a particular complication arises for harmonic shape functions and their corresponding $C^0(\Omega)$ approximations on irregularly shaped elements: the solution to Laplace's equation may possess extremely sharp gradients if the geometry of the element contains reflex corners or nearly degenerate features (i.e. short edges). A consequence of this is poor conditioning of the element's local stiffness matrix, leading to excessively stiff modes

of deformation (locking), and issues of numerical conditioning in the linear solution process. For this reason, it becomes of interest to consider non-conforming approximations $\varphi^h \in \mathcal{U}^h(\Omega) \not\subset \mathcal{U}(\Omega)$ which have the potential to overcome these issues.

Non-conforming Galerkin Approximations to Generalized Harmonic Shape Functions

If the boundary conditions imposed upon a given shape function are relaxed to the extent that $\varphi^h \neq \bar{\varphi}$ on $\partial\Omega$, then clearly $\mathcal{U}^h(\Omega) \not\subset \mathcal{U}(\Omega)$, and one must resort to the use of non-conforming approximation methods. In such cases, the boundary conditions must be imposed in a weak sense, such that φ^h still converges to φ as the dimension of the non-conforming approximation space $\mathcal{U}^h(\Omega)$ is increased. A number of potential weak enforcement strategies are suggested in the following sections.

Weak Enforcement of Boundary Conditions via a Lagrange Multiplier Method

One possible approach would be to consider a Lagrange multiplier method, to weakly enforce the boundary condition $\varphi = \bar{\varphi}$ on $\partial\Omega$ via

$$\min_{\varphi,\,\lambda} \mathcal{L}(\varphi, \lambda), \tag{3.16}$$

$$\mathcal{L}(\varphi, \lambda) \equiv \frac{1}{2}\int_\Omega \nabla\varphi \cdot \nabla\varphi \, dV - \int_\Omega f_\Omega \, \varphi \, dV + \int_{\partial\Omega} [\varphi - \bar{\varphi}] \, \lambda \, dA, \tag{3.17}$$

involving the specification of a Lagrange multiplier field $\lambda \in \Lambda(\partial\Omega) = \{\lambda \in L^2(\partial\Omega)\}$, and it's corresponding approximation $\lambda^h \in \Lambda^h(\partial\Omega) \subset \Lambda(\partial\Omega)$. Differentiation of the Lagrangian yields two sets of equations in terms of the approximations $\varphi^h \in \mathcal{U}^h(\Omega)$ and $\lambda^h \in \Lambda^h(\partial\Omega)$:

$$\int_\Omega \nabla\varphi^h \cdot \nabla\eta^h \, dV - \int_\Omega f_\Omega \eta^h \, dV + \int_{\partial\Omega} \lambda^h \eta^h \, dA = 0 \quad \forall \eta^h \in \mathcal{U}^h(\Omega), \tag{3.18}$$

$$\int_{\partial\Omega} (\varphi^h - \bar{\varphi}) \, \mu^h \, dA = 0 \quad \forall \mu^h \in \Lambda^h(\partial\Omega). \tag{3.19}$$

Suppose finite-dimensional bases are established for $\mathcal{U}^h(\Omega)$ and $\Lambda^h(\partial\Omega)$, i.e.

$$\varphi^h(\mathbf{X}) = \sum_{a=1}^{N} \psi_a(\mathbf{X})\varphi_a, \quad \lambda^h(\mathbf{X}) = \sum_{a=1}^{M} \chi_a(\mathbf{X})\lambda_a, \tag{3.20}$$

such that

$$\sum_{a=1}^{N}\left[\int_{\Omega}\nabla\psi_a\cdot\nabla\psi_b\,dV\right]\varphi_a+\sum_{c=1}^{M}\left[\int_{\partial\Omega}\psi_b\,\chi_c\,dA\right]\lambda_c=\int_{\partial\Omega}f_\Omega\,\psi_b\,dA\quad\forall b, \tag{3.21}$$

$$\sum_{b=1}^{N}\left[\int_{\partial\Omega}\chi_c\,\psi_b\,dA\right]\varphi_b=\int_{\partial\Omega}\bar{\varphi}\,\chi_c\,dA\quad\forall c. \tag{3.22}$$

Given an appropriate selection for the indicated bases, the determination of the unknowns (φ_a and λ_a) entails the solution of a saddle-point system of equations, written in matrix-vector format:

$$\begin{bmatrix}\mathbf{A} & \mathbf{B}\\ \mathbf{B}^T & \mathbf{0}\end{bmatrix}\begin{Bmatrix}\boldsymbol{\varphi}\\ \boldsymbol{\lambda}\end{Bmatrix}=\begin{Bmatrix}\mathbf{f}\\ \bar{\boldsymbol{\varphi}}\end{Bmatrix}, \tag{3.23}$$

where

$$A_{ab}=\int_{\Omega}\nabla\psi_a\cdot\nabla\psi_b\,dV,\quad B_{bc}=\int_{\partial\Omega}\psi_b\,\chi_c\,dA, \tag{3.24}$$

$$f_b=\int_{\partial\Omega}f_\Omega\,\psi_b\,dA,\quad\bar{\varphi}_c=\int_{\partial\Omega}\bar{\varphi}\,\chi_c\,dA. \tag{3.25}$$

The main advantage of this approach is that virtually any space of functions may be selected for $\mathcal{U}^h(\Omega)$, such that the resulting approximations $\varphi^h\in\mathcal{U}^h(\Omega)$ deliberately do not contain sharp gradients.

Arguably the simplest (and most efficient) choice is $\mathcal{U}^h(\Omega)=P^k(\Omega)$, resembling certain formulations of the VETFEM ([36], [38]) where the basis functions for the Lagrange multiplier field $\chi_c(\mathbf{X})=\delta(\mathbf{X}-\mathbf{X}_c)\ \forall c=1,\ldots,N_v$ are Dirac delta functions associated with the individual nodes of the element. A potential shortcoming of this particular choice for χ_c is that the resulting shape functions may yield sharp gradients along short element edges.

Various other choices for the Lagrange multiplier basis are possible which may yield less spurious solutions (for instance $\Lambda^h(\partial\Omega)=P^k(\partial\Omega)$), though these may lead to ill-posedness of the saddle-point problem. More sophisticated linear solution methodologies are required in these cases.

Weak Enforcement of Boundary Conditions via Nitsche's Method

As a viable alternative to the Lagrange multiplier method presented in the previous section, one may instead consider using Nitsche's method (refer to [25]) as a means of

weakly enforcing the boundary conditions for a given shape function, i.e.

$$\int_\Omega \nabla\varphi^h \cdot \nabla\eta^h \, dV - \int_{\partial\Omega} \left[\frac{\partial\varphi^h}{\partial N}\eta^h + \varphi^h \frac{\partial\eta^h}{\partial N} \right] dA + \frac{1}{\gamma|\partial\Omega|^\beta} \int_{\partial\Omega} \varphi^h \eta^h \, dA$$
$$= \int_\Omega f_\Omega \, \eta^h \, dV - \int_{\partial\Omega} \bar{\varphi} \frac{\partial\eta^h}{\partial N} \, dA + \frac{1}{\gamma|\partial\Omega|^\beta} \int_{\partial\Omega} \bar{\varphi}\eta^h \, dA \quad \forall \eta^h \in \mathcal{U}^h(\Omega), \tag{3.26}$$

where $\gamma > 0$ is a stabilization parameter, $|\partial\Omega|$ denotes the surface area of $\partial\Omega$, and $\beta = (d-1)^{-1}$ for $\Omega \subset \mathbb{R}^d$, $d \geq 2$.

Provided the stabilization parameter γ is specified appropriately, the Galerkin approximation φ^h to Nitsche's method can be obtained as the solution to the symmetric, positive-definite system of equations $\mathbf{A}\boldsymbol{\varphi} = \mathbf{f}$, where

$$A_{ab} = \int_\Omega \nabla\psi_a \cdot \nabla\psi_b \, dV - \int_{\partial\Omega} \left[\frac{\partial\psi_a}{\partial N}\psi_b + \psi_a \frac{\partial\psi_b}{\partial N} \right] dA + \frac{1}{\gamma|\partial\Omega|^\beta} \int_{\partial\Omega} \psi_a \, \psi_b \, dA, \tag{3.27}$$

$$f_b = \int_\Omega f_\Omega \, \psi_b \, dV - \int_{\partial\Omega} \bar{\varphi} \frac{\partial\psi_b}{\partial N} \, dA + \frac{1}{\gamma|\partial\Omega|^\beta} \int_{\partial\Omega} \bar{\varphi} \, \psi_b \, dA. \tag{3.28}$$

As discussed in the previous section, a rather natural choice for the space of approximating functions is $\mathcal{U}^h(\Omega) = P^k(\Omega)$. The resulting method yields reasonably well-conditioned stiffness matricies for convex shapes, even when the elements possess degenerate edges. However, experimental evidence suggests that for non-convex shapes, the resulting shape function approximations may succumb to Runge's phenomenon. Figure (L) depicts the results for increasing k.

These considerations have led to the conclusion that piecewise approximation methods may provide a preferred means for constructing more well-behaved approximations. The remainder of our discussion will focus upon such methods.

3.4 Piecewise Polynomial Approximations to Generalized Harmonic Shape Functions

Partitioned element methods consider the approximation to a given element's shape functions via piecewise polynomials defined over a partition of the element's domain. In this regard, the approach proposed by Bishop in [4] is properly regarded as a partitioned element method.

The eponymous partitioned element method introduced in [37] solves (3.9) by empolying an approximation scheme which closely resembles a stabilized virtual element method. Herein we propose an alternative approach based upon the interior penalty discontinuous Galerkin finite element method.

The Element Partition

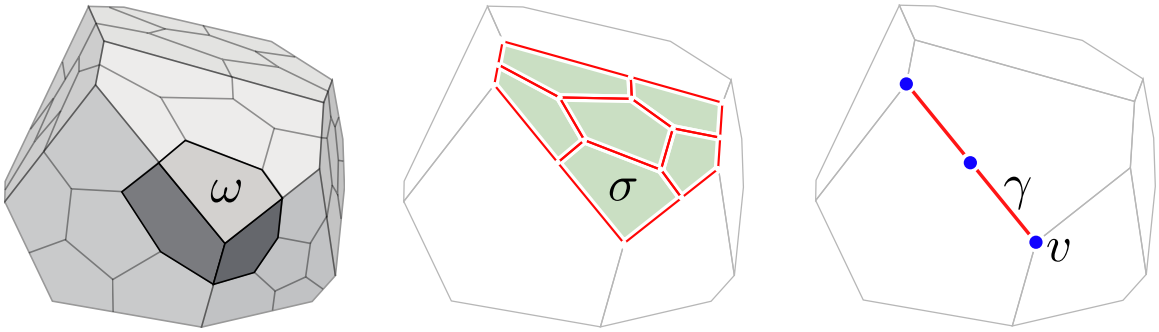

Figure 3.4. A representative polyhedral element $\Omega \subset \mathbb{R}^3$, and it's corresponding partition into cells, facets, segments, and verticies.

Consider a partition $\mathcal{T}_\omega(\Omega)$ of a given polyhedral element Ω into polyhedral cells $\omega \subset \Omega$. The boundary of each cell consists of polygonal facets $\sigma \subset \partial\omega$. Further, denote by Γ_ω the set of all interior cell interfaces (facets) shared by two adjacent cells, such that a given polygonal facet σ belongs either to Γ_ω or the boundary of the element $\partial\Omega$.

In turn, let $\mathcal{T}_\sigma(F)$ denote the partition of a given face $F \subset \partial\Omega$ into polygonal facets $\sigma \subset F$. The boundary of each facet consists of linear segments $\gamma \subset \partial\sigma$. For each face F, Γ_σ shall denote the set of all interior facet interfaces (segments) shared by two facets belonging to F, such that a given linear segment γ belongs either to Γ_σ or ∂F.

Finally, $\mathcal{T}_\gamma(E)$ denotes the partition of a given edge $E \subset \partial F$ into linear segments $\gamma \subset E$. The endpoints of each segment are called verticies $v \subset \partial\gamma$. For each edge E, Γ_γ denotes the set of all interior segment interfaces (verticies) shared by two segments belonging to E, such that a given vertex v belongs either to Γ_γ or ∂E. Any vertex $v \in \partial E$ is also a node $v = V$.

Several simple partitioning schemes are proposed:

- **Edge-based**: For star-convex shapes – the vertex-averaged centroid is used to subdivide the element into triangles (in 2D) or tetrahedra (in 3D) which are associated

with each linear edge of the element.

- **Node-based**: For arbitrary shapes – the element is sub-divided into quadrature cells corresponding to the tributary area surrounding each node.

- **Voronoi**: For arbitrary shapes – the element is sub-divided into Voronoi cells, whose corresponding voronoi sites are generated via a constrained maximal poisson-disk sampling process, as described in [15].

The aforementioned approaches are further illustrated in Figure 3.5.

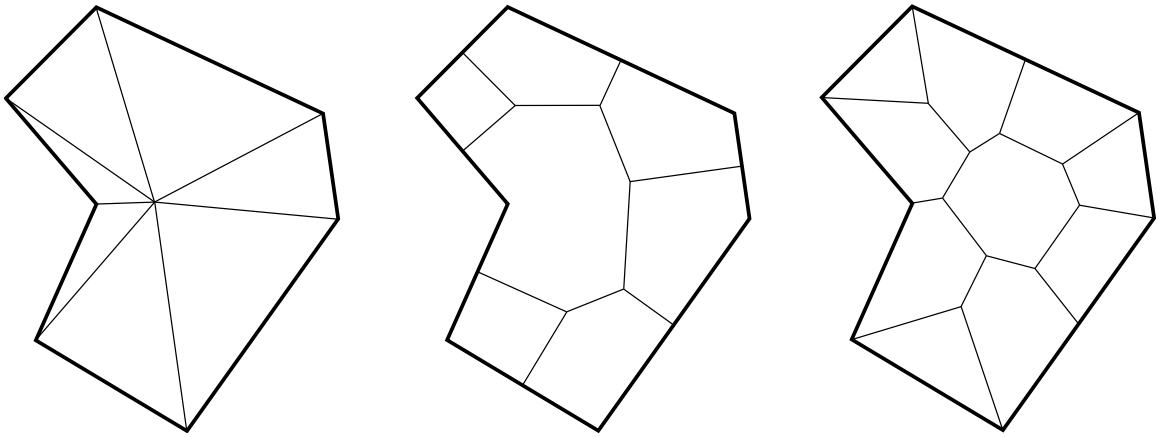

Figure 3.5. Polygonal element partitioning schemes, from left to right: edge-based partition, node-based partition, voronoi partition.

We denote the volume of a given cell as $|\omega|$, the area of a facet as $|\sigma|$, and the length of a segment as $|\gamma|$. Each facet possesses an associated normal direction $\mathbf{N}_\sigma$, whose orientation is outward from Ω for all $\sigma \in \partial\Omega$. The orientation of $\mathbf{N}_\sigma$ is otherwise arbitrary for all $\sigma \in \Gamma_\omega$. Likewise,

Discontinuous Galerkin Approximations to Harmonic Shape Functions

Consider the broken Sobolev space $\mathcal{D}_k^h(\Omega) = \left\{\varphi \in L^2(\Omega) : \varphi|_\omega \in P^k(\omega)\, \forall \omega \in \mathcal{T}_\omega(\Omega)\right\}$ consisting of (discontinuous) piecewise polynomials defined over the partition of the element. The symmetric interior penalty discontinuous Galerkin method (SIPG) described in [40] is applied to (3.8) to obtain approximations $\varphi^h \in \mathcal{D}_k^h(\Omega) \not\subset \mathcal{U}(\Omega)$ to generalized harmonic

shape functions $\varphi \in \mathcal{U}(\Omega)$, satisfying

$$\sum_{\omega\in\mathcal{T}_\omega(\Omega)} \int_\omega \nabla\varphi^h \cdot \nabla\eta^h \, dV - \sum_{\sigma\in\Gamma_\omega\cup\partial\Omega} \int_\sigma \left(\left\{ \frac{\partial\varphi^h}{\partial N_\sigma} \right\} [\![\eta^h]\!] + [\![\varphi^h]\!] \left\{ \frac{\partial\eta^h}{\partial N_\sigma} \right\} \right) dA$$
$$+ J_0(\varphi^h, \eta^h) + J_1(\varphi^h, \eta^h) = \int_\Omega f_\Omega \, \eta^h \, dV + \sum_{\sigma\in\partial\Omega} \int_\sigma \left(\frac{\alpha_{\sigma 0}}{|\sigma|^{\beta_0}} \eta^h - \frac{\partial\eta^h}{\partial N_\sigma} \right) \bar{\varphi} \, dA \qquad (3.29)$$

for all $\eta^h \in \mathcal{D}_k^h(\Omega)$, where

$$\{\varphi\} = \frac{1}{2}(\varphi|_{\omega_1} + \varphi|_{\omega_2}), \quad [\![\varphi]\!] = (\varphi|_{\omega_1} - \varphi|_{\omega_2}) \quad \forall\sigma = \partial\omega_1 \cap \partial\omega_2, \qquad (3.30)$$

$$\{\varphi\} = [\![\varphi]\!] = \varphi|_\omega \quad \forall\sigma = \partial\omega \cap \partial\Omega, \qquad (3.31)$$

and where

$$J_0(\varphi^h, \eta^h) = \sum_{\sigma\in\Gamma_\omega\cup\partial\Omega} \frac{\alpha_{\sigma 0}}{|\sigma|^{\beta_0}} \int_\sigma [\![\varphi^h]\!] \, [\![\eta^h]\!] \, dA, \qquad (3.32)$$

$$J_1(\varphi^h, \eta^h) = \sum_{\sigma\in\Gamma_\omega} \frac{\alpha_{\sigma 1}}{|\sigma|^{\beta_1}} \int_\sigma \left[\!\!\left[\frac{\partial\varphi^h}{\partial N_\sigma} \right]\!\!\right] \left[\!\!\left[\frac{\partial\eta^h}{\partial N_\sigma} \right]\!\!\right] dA. \qquad (3.33)$$

$J_0(\varphi^h, \eta^h)$ and $J_1(\varphi^h, \eta^h)$ are supplementary bilinear forms which penalize jumps in the indicated functions' values and their normal derivatives at cell boundaries. The parameters $\alpha_{\sigma 0}$, β_0, must be appropriately specified such that $\alpha_{\sigma 0} > 0$ is sufficiently large, and $\beta_0(d-1) \geq 1$ where $\Omega \subset \mathbb{R}^d$, $d \geq 2$; the specification of $\alpha_{\sigma 1}$, β_1 is less strict, allowing for $\alpha_{\sigma 1} \geq 0 \ \forall\sigma$.

If one considers a non-dimensional analysis where $\mathbf{X} = h_\Omega \mathbf{X}'$, and h_Ω denotes a characteristic length scale corresponding to the diameter of the element Ω, the following quantities may be expressed in terms of their non-dimensional counterparts:

$$dV = h_\Omega^d dV', \quad dA = h_\Omega^{d-1} dA', \quad \nabla = h_\Omega^{-1}\nabla', \quad |\sigma| = h_\Omega^{d-1}|\sigma'|, \quad f_\Omega = h_\Omega^{-2} f_{\Omega'}. \qquad (3.34)$$

It is presumed that $\alpha_{\sigma 0}$, $\alpha_{\sigma 1}$ are defined independently of h_Ω. Consequently,

$$h_\Omega^{d-2}\left[\sum_{\omega'\in\mathcal{T}_{\omega'}(\Omega')}\int_{\omega'}\nabla'\varphi^h\cdot\nabla'\eta^h\,dV'-\int_{\Omega'}f_{\Omega'}\,\eta^h\,dV'+\sum_{\sigma'\in\partial\Omega'}\int_{\sigma'}\frac{\partial\eta^h}{\partial N_{\sigma'}}\,\bar{\varphi}\,dA'\right.$$
$$\left.-\sum_{\sigma'\in\Gamma_{\omega'}\cup\partial\Omega'}\int_{\sigma'}\left(\left\{\frac{\partial\varphi^h}{\partial N_{\sigma'}}\right\}[\![\eta^h]\!]+[\![\varphi^h]\!]\left\{\frac{\partial\eta^h}{\partial N_{\sigma'}}\right\}\right)dA'\right]$$
$$+h_\Omega^{(d-1)(1-\beta_0)}\left[\sum_{\sigma'\in\Gamma_{\omega'}\cup\partial\Omega'}\frac{\alpha_{\sigma 0}}{|\sigma'|^{\beta_0}}\int_{\sigma'}[\![\varphi^h]\!]\,[\![\eta^h]\!]\,dA'-\sum_{\sigma'\in\partial\Omega'}\frac{\alpha_{\sigma 0}}{|\sigma'|^{\beta_0}}\int_{\sigma'}\eta^h\,\bar{\varphi}\,dA'\right]$$
$$+h_\Omega^{(d-1)(1-\beta_1)-2}\left[\sum_{\sigma'\in\Gamma_{\omega'}}\frac{\alpha_{\sigma 1}}{|\sigma'|^{\beta_1}}\int_{\sigma'}\left[\!\left[\frac{\partial\varphi^h}{\partial N_{\sigma'}}\right]\!\right]\,\left[\!\left[\frac{\partial\eta^h}{\partial N_{\sigma'}}\right]\!\right]\,dA'\right]=0\quad\forall\eta^h\in\mathcal{D}_k^h(\Omega).\tag{3.35}$$

To maintain dimensional consistency, it is suggested that β_0 and β_1 be chosen such that

$$\beta_0=(d-1)^{-1},\quad\beta_1=-(d-1)^{-1}.\tag{3.36}$$

To ensure that the resulting linear system of equations is reasonably well-conditioned, the penalty parameters $\alpha_{\sigma 0}$, $\alpha_{\sigma 1}$ should not be made excessively large. Nonetheless, an interesting limiting case occurs when $\alpha_{\sigma 0},\alpha_{\sigma 1}\to\infty$ proportionally:

$$J_0(\varphi^h,\eta^h)+J_1(\varphi^h,\eta^h)=\sum_{\sigma\in\partial\Omega}\frac{\alpha_{\sigma 0}}{|\sigma|^{\beta_0}}\int_\sigma\eta^h\,\bar{\varphi}\,dA\quad\forall\eta^h\in\mathcal{D}_k^h(\Omega).\tag{3.37}$$

Under certain conditions (for particular choices of $\mathcal{T}_\omega(\Omega)$ and $\mathcal{D}_k^h(\Omega)$), the above weak form may in fact yield a unique solution φ^h. However, the bilinear form arising from the penalty terms J_0 and J_1 alone is not guaranteed to be elliptic, in general.

The majority of our subsequent analyses will explore the family of 3-parameter methods arising from

$$\alpha_{\sigma 0}=\alpha_0|_{\partial\Omega}\;\forall\sigma\in\partial\Omega,\quad\alpha_{\sigma 0}=\alpha_0|_{\Gamma_\omega}\;\forall\sigma\in\Gamma_\omega,\quad\alpha_{\sigma 1}=\alpha_1|_{\Gamma_\omega}\;\forall\sigma\in\Gamma_\omega,\tag{3.38}$$

entailing a separate penalization of the boundary condition via $\alpha_0|_{\partial\Omega}$. Decreasing the value of $\alpha_0|_{\partial\Omega}$ is tantamount to relaxing the degree to which the boundary condition is enforced, the effect of which will be examined and discussed later on.

3.5 Partition-Based Quadrature Rules

If arbitrary polytopal shapes are to be used as elements in the PEM, then there arises a need for devising a means of integrating contributions to the weak form, ostensibly through the use of domain quadrature rules. Such rules must be sufficiently stable (utilizing a sufficient number of well-positioned quadrature points) and accurate (capable of exactly integrating low-order polynomials up to some specified degree).

Partitioned element methods approach this task by partitioning the elements (and their boundaries) into a sufficient number of polytopal sub-domains which are used as integration cells. Low-order (i.e. 1-point) quadrature rules are defined on each of these sub-domains, and a composite quadrature rule for the element is constructed from the resulting sets of quadrature points. In general, these rules will need to be modified to satisfy Galerkin exactness for certain low-order polynomial solutions.

Methods for partitioning the elements into sub-domains which yield stable and efficient composite quadrature rules are discussed in the following section. A discussion is given later on to the correction of these quadratures for the sake of satisfying Galerkin exactness (quadrature consistency).

Composite Quadrature Rules

Given a partition of an element into polytopal sub-domains (quadrature cells), one may utilize low order quadrature rules over each sub-domain, thereby yielding a composite quadrature rule over the element as a whole, whose overall accuracy is determined by the order of accuracy used in each sub-domain.

The simplest quadrature rule of this form is the composite mid-point scheme, where the quadrature points are located at the centroids of each sub-domain. Such a rule exactly integrates polynomials up to first order, and is reasonably accurate, otherwise. The integration points are guaranteed to be interior to each sub-domain (and the element as a whole), provided each cell is convex.

For simple sub-divisions (consisting of triangles or tetrahedra), composite quadrature rules may be extended rather naturally to obtain higher-order accuracy. For generic sub-divisions (consiting of arbitrary polytopes), the extension to high-order is not as straight-

forward. For this reason, subsequent discussions will be concerned almost exclusively with composite mid-point rules.

The weights and locations of a composite mid-point quadrature rule correspond to the volumes and geometric centroids of each cell. In general, a given quadrature cell ω may be an arbitrary polyhedron, whose volume $|\omega|$ and centroid $\bar{\mathbf{X}}$ may be computed using the 0-th and 1-st order moments of ω, i.e.

$$|\omega| = \int_\omega dV, \quad \bar{\mathbf{X}} = \frac{\int_\omega \mathbf{X}\, dV}{\int_\omega dV}. \tag{3.39}$$

Using the method proposed by Chin et al. in [9], the computation of monomial moments of arbitrary degree $|\alpha|$ may be effected via an integral over $\partial\omega$:

$$\int_\omega \mathbf{X}^\alpha\, dV = \frac{1}{d+|\alpha|} \int_{\partial\omega} (\mathbf{X}\cdot\mathbf{N})\, \mathbf{X}^\alpha\, dA, \tag{3.40}$$

for any arbitrary polytope $\omega \subset \mathbb{R}^d$. If $\partial\omega$ may be partitioned into a collection of $d-1$ dimensional facets $\sigma \subset \partial\omega$, then

$$\int_\omega \mathbf{X}^\alpha\, dV = \frac{1}{d+|\alpha|} \sum_{\sigma\in\partial\omega} \int_\sigma (\mathbf{X}\cdot\mathbf{N}_\sigma)\, \mathbf{X}^\alpha\, dA, \tag{3.41}$$

where $\mathbf{N}_\sigma$ is the outward (with respect to ω) unit normal associated with facet σ. We remark that any location $\mathbf{X}$ positioned on a given facet σ may be expressed as

$$\mathbf{X} = \mathbf{X}_\sigma + \sum_{i=1}^{d-1} X_i\, \hat{\mathbf{X}}_i, \tag{3.42}$$

where $\mathbf{X}_\sigma$ is any reference location positioned on the hyperplane which contains σ, and $\hat{\mathbf{X}}_i$ form a parameterization of the in-plane coordinates on σ. This leads to the observation $\mathbf{X}\cdot\mathbf{N}_\sigma = \mathbf{X}_\sigma\cdot\mathbf{N}_\sigma\ \forall\mathbf{X}\in\sigma$, and thus

$$\int_\omega \mathbf{X}^\alpha\, dV = \frac{1}{d+|\alpha|} \sum_{\sigma\in\partial\omega} (\mathbf{X}_\sigma\cdot\mathbf{N}_\sigma) \int_\sigma \mathbf{X}^\alpha\, dA. \tag{3.43}$$

The integral of $\mathbf{X}^\alpha$ over each facet may in turn be carried out via

$$\int_\sigma \mathbf{X}^\alpha\, dA = \frac{1}{d-1+|\alpha|} \left[\sum_{\gamma\in\partial\sigma} \left((\mathbf{X}_\gamma - \mathbf{X}_\sigma)\cdot\mathbf{N}_\gamma\right) \int_\gamma \mathbf{X}^\alpha\, dS + \mathbf{X}_\sigma \cdot \int_\sigma \nabla\mathbf{X}^\alpha\, dA \right], \tag{3.44}$$

and the integral over each segment is

$$\int_\gamma \mathbf{X}^\alpha \, dS = \frac{1}{d-2+|\alpha|} \left[\sum_{v \in \partial\gamma} \big((\mathbf{X}_v - \mathbf{X}_\gamma) \cdot \mathbf{N}_v \big) \mathbf{X}_v^\alpha + \mathbf{X}_\gamma \cdot \int_\gamma \nabla \mathbf{X}^\alpha \, dS \right]. \tag{3.45}$$

This process may be applied recursively to ultimately reduce the monomial integrals over ω to weighted vertex evaluations (or edge integrals, as one prefers).

Similarly defined composite rules may be defined on each polygonal face of a given polyhedral element, or on each edge of a polygonal element. However, while composite mid-point quadrature rules are able to provide reasonable accuracy, they will not necessarily lead to quadrature consistency, as expressed in (2.67). For this reason, a gradient correction scheme (such as the one proposed by Bishop in [4], or by Talischi in [50]) must be employed. Alternatively, a novel approach to restore quadrature consistency is presented in the following section.

Selective Modal Quadrature

Consider all functions $f \in L^2(\Omega)$ represented over an arbitrary polytopal element domain $\Omega \subset \mathbb{R}^d$. Standard quadrature rules approximate the integral of f over Ω as

$$\int_\Omega f \, dV \approx \sum_{q=1}^{N_{qp}} w_q f(\mathbf{x}_q). \tag{3.46}$$

Borrowing from notation typical of the VEM, consider an $L^2(\Omega)$ polynomial projection operator $\Pi_k^\Omega : L^2(\Omega) \mapsto P^k(\Omega)$ which may be used to decompose $f = f_p + f_n$ into polynomial and non-polynomial parts:

$$f_p = \Pi_k^\Omega f, \quad f_n = f - \Pi_k^\Omega f = \pi_k^\Omega f, \tag{3.47}$$

where $\pi_k^\Omega : L^2(\Omega) \mapsto L^2(\Omega) \backslash P^k(\Omega)$. Consequently, we observe that $\Pi_k^\Omega f$ is $L^2(\Omega)$ orthogonal to any $\pi_k^\Omega g$ for all $g \in L^2(\Omega)$, to the extent that

$$\int_\Omega (\Pi_k^\Omega f)(g - \Pi_k^\Omega g) \, dv = \langle \Pi_k^\Omega f, g - \Pi_k^\Omega g \rangle_\Omega = 0 \quad \forall f,\, g \in L^2(\Omega). \tag{3.48}$$

We propose a quadrature rule of the form:

$$\int_\Omega f \, dV \approx \int_\Omega f_p \, dV + \sum_{q=1}^{N_{qp}} w_q f_n(\mathbf{x}_q), \tag{3.49}$$

where it is supposed that the projection operators Π_k^Ω and π_k^Ω are well-defined on Ω, and $\int_\Omega f_p \, dV$ may be computed exactly using the methodology proposed by Chin et al. in [9]. Furthermore, if we wish to integrate the product fg where $f,\, g \in L^2(\Omega)$, we may write

$$\int_\Omega fg \, dV = \langle f, g \rangle_\Omega = \langle \Pi_k^\Omega f + \pi_k^\Omega f, \Pi_k^\Omega g + \pi_k^\Omega g \rangle_\Omega, \tag{3.50}$$

which, by the linearity of the $L^2(\Omega)$ inner product, and by the orthogonality of $\Pi_k^\Omega f$ and $\pi_k^\Omega g$ (and of $\pi_k^\Omega f$ and $\Pi_k^\Omega g$), yields

$$\int_\Omega fg \, dV = \langle \Pi_k^\Omega f, \Pi_k^\Omega g \rangle_\Omega + \langle \pi_k^\Omega f, \pi_k^\Omega g \rangle_\Omega, \tag{3.51}$$

and thus

$$\int_\Omega fg \, dV \approx \int_\Omega f_p g_p \, dV + \sum_{q=1}^{N_{qp}} w_q f_n(\mathbf{x}_q) g_n(\mathbf{x}_q). \tag{3.52}$$

This is effectively equivalent to integrating the product of all low-order polynomials exactly, while integrating the product of all non-polynomial "remainders" approximately, using a quadrature rule.

If we are only given evaluations of a function f at a set of discrete (quadrature) points $\{\mathbf{x}_q\}_{q=1}^{N_{qp}}$, then we must construct a low-order polynomial projection operator by considering the least-squares problem:

$$\min_{f_p \in P^k(\Omega)} \frac{1}{2} ||f_p - f||_\Omega^2, \tag{3.53}$$

where $||f||_\Omega = \sqrt{\langle f, f \rangle_\Omega}$ is deliberately approximated using the element's quadrature rule:

$$\langle f, f \rangle_\Omega \approx \sum_{q=1}^{N_{qp}} w_q \left[f(\mathbf{x}_q) \right]^2. \tag{3.54}$$

For a given polynomial basis $\{z_a\}_{a=1}^K$ which spans $P^k(\Omega)$, we may write

$$f_p(\mathbf{x}) = \sum_{a=1}^{K} z_a(\mathbf{x}) c_a = \mathbf{z}^T(\mathbf{x}) \, \mathbf{c}, \tag{3.55}$$

and the solution to (3.54) satisfies

$$\sum_{a=1}^{K} \sum_{q=1}^{N_{qp}} w_q z_b(\mathbf{x}_q) z_a(\mathbf{x}_q) c_a = \sum_{q=1}^{N_{qp}} w_q z_b(\mathbf{x}_q) f(\mathbf{x}_q) \quad \forall b = 1, \ldots, K, \tag{3.56}$$

The above may be written in matrix-vector format as $\mathbf{Z}^T\mathbf{W}\mathbf{Z}\mathbf{c} = \mathbf{Z}^T\mathbf{W}\mathbf{f}$, where we denote $f_i = f(\mathbf{x}_i)$, $W_{ii} = w_i$, $W_{ij} = 0\,\forall i \neq j$, and $Z_{ij} = z_j(\mathbf{x}_i)$. The discrete polynomial projection operator $\mathbf{\Pi}_k^\Omega : \mathbb{R}^{N_{qp}} \mapsto \mathbb{R}^K$ is computed as $\mathbf{\Pi}_k^\Omega = (\mathbf{Z}^T\mathbf{W}\mathbf{Z})^{-1}\mathbf{Z}^T\mathbf{W}$, and the complement operator $\boldsymbol{\pi}_k^\Omega : \mathbb{R}^{N_{qp}} \mapsto \mathbb{R}^{N_{qp}}$ is $\boldsymbol{\pi}_k^\Omega = \mathbf{1}_{N_{qp}} - \mathbf{Z}\mathbf{\Pi}_k^\Omega$. Consequently,

$$\langle \Pi_k^\Omega f, \Pi_k^\Omega g \rangle_\Omega = \langle \mathbf{z}^T\mathbf{\Pi}_k^\Omega\mathbf{f}, \mathbf{z}^T\mathbf{\Pi}_k^\Omega\mathbf{g} \rangle_\Omega = \mathbf{f}^T \left[\mathbf{\Pi}_k^{\Omega^T} \left(\int_\Omega \mathbf{z} \otimes \mathbf{z}\, dV \right) \mathbf{\Pi}_k^\Omega \right] \mathbf{g}, \tag{3.57}$$

$$\langle \pi_k^\Omega f, \pi_k^\Omega g \rangle_\Omega \approx \sum_{q=1}^{N_{qp}} w_q f_n(\mathbf{x}_q) g_n(\mathbf{x}_q) = \mathbf{f}^T \left[\boldsymbol{\pi}_k^{\Omega^T} \mathbf{W} \boldsymbol{\pi}_k^\Omega \right] \mathbf{g}, \tag{3.58}$$

and thus

$$\int_\Omega f g\, dV \approx \mathbf{f}^T \mathbf{M}_k \mathbf{g} = \sum_{q=1}^{N_{qp}} \sum_{p=1}^{N_{qp}} M_k(\mathbf{x}_q, \mathbf{x}_p)\, f(\mathbf{x}_q)\, g(\mathbf{x}_p), \tag{3.59}$$

$$\mathbf{M}_k \equiv \left[\mathbf{\Pi}_k^{\Omega^T} \left(\int_\Omega \mathbf{z} \otimes \mathbf{z}\, dV \right) \mathbf{\Pi}_k^\Omega \right] + \left[\boldsymbol{\pi}_k^{\Omega^T} \mathbf{W} \boldsymbol{\pi}_k^\Omega \right]. \tag{3.60}$$

We shall refer to this form of integration as *selective modal quadrature*, given that the products of particular low-order polynomial modes are integrated exactly, and the products of any higher-order modes are approximated using the element's quadrature rules. The advantage of modal quadrature is that we may exactly integrate any terms which directly impact quadrature consistency. Consequently, nearly any stable numerical integration scheme (e.g. composite mid-point quadrature) may be used to integrate the higher-order products.

Rather than storing the independent quadrature weights $w_q = w(\mathbf{x}_q)$, selective modal quadrature requires the storage of a generalized quadrature weighting matrix $M_k(\mathbf{x}_q, \mathbf{x}_p)$. Alternatively, for the sake of efficiency, if the function g is known a priori (e.g. if g is a test function for a weighted residual method), then we need only store the "augmented" test function values:

$$\tilde{g}^{(k)}(\mathbf{x}_q) = \sum_{p=1}^{N_{qp}} \frac{M_k(\mathbf{x}_q, \mathbf{x}_p)}{w_q}\, g(\mathbf{x}_p), \tag{3.61}$$

and all integrals involving f and g may be carried out via

$$\int_\Omega f g\, dV \approx \sum_{q=1}^{N_{qp}} w_q\, \tilde{g}^{(k)}(\mathbf{x}_q)\, f(\mathbf{x}_q). \tag{3.62}$$

If applied to the stress divergence integral appearing in (2.39), the resulting expression would resemble a gradient correction scheme in some respects, although it should be noted that the above procedure would need to be applied separately to each term appearing in the weak form (including boundary integrals). Specifically, the corresponding integration of the residual equations in (2.39) would be carried out via

$$\int_{\mathcal{B}_0} P_{ij}\phi_{a,j}\,dV \approx \sum_{q=1}^{N_{qp}} w_q P_{ij}(\mathbf{x}_q)\tilde{\phi}^{(k)}_{a,j}(\mathbf{x}_q), \tag{3.63}$$

$$\int_{\mathcal{B}_0} \rho_0 b_i\phi_a\,dV \approx \sum_{q=1}^{N_{qp}} w_q \rho_0(\mathbf{x}_q) b_i(\mathbf{x}_q)\tilde{\phi}^{(k-1)}_{a}(\mathbf{x}_q), \tag{3.64}$$

$$\int_{\Gamma_0^N} \bar{p}_i\phi_a\,dA \approx \sum_{b=1}^{N_{bp}} w_b \bar{p}_i(\mathbf{x}_b)\tilde{\phi}^{(k)}_{a}(\mathbf{x}_b), \tag{3.65}$$

where $\tilde{\phi}^{(k)}_a$ and $\tilde{\phi}^{(k)}_{a,j}$ denote the "augmented" test functions are their corresponding gradients, and k is the indicated order of quadrature consistency (required to pass patch tests up to order $k+1$).

References

[1] Ivo Babuška. Error-bounds for finite element method. *Numerische Mathematik*, 16:322–333, 1971.

[2] Ivo Babuška and Manil Suri. Locking effects in the finite element approximation of elasticity problems. *Numerische Mathematik*, 62:439–463, 1992.

[3] Ivo Babuška and Manil Suri. On locking and robustness in the finite element method. *SIAM Journal on Numerical Analysis*, 29(5):1261–1293, 1992.

[4] J. E. Bishop. A displacement-based finite element formulation for general polyhedra using harmonic shape functions. *International Journal for Numerical Methods in Engineering*, 97:1–31, 2014.

[5] Franco Brezzi. On the existence, uniqueness and approximation of saddle-point problems arising from lagrangian multipliers. *ESAIM: Mathematical Modelling and Numerical Analysis - Modlisation Mathmatique et Analyse Numrique*, 8:129–151, 1974.

[6] Jiun-Shyan Chen, Michael Hillman, and Marcus Rüter. An arbitrary order variationally consistent integration for galerkin meshfree methods. *International Journal for Numerical Methods in Engineering*, 95:387–418, 2013.

[7] H. Chi, L. Beirão da Veiga, and G. H. Paulino. Some basic formulations of the virtual element method (vem) for finite deformations. *Computer Methods in Applied Mechanics and Engineering*, 318:148–192, 2017.

[8] Heng Chi, Cameron Talischi, Oscar Lopez-Pamies, and Glaucio H. Paulino. A paradigm for higher-order polygonal elements in finite elasticity using a gradient correction scheme. *Computer Methods in Applied Mechanics and Engineering*, 306:216–251, 2016.

[9] Eric B. Chin, Jean B. Lasserre, and N. Sukumar. Numerical integration of homogeneous functions on convex and nonconvex polygons and polyhedra. *Computational Mechanics*, 56:967–981, 2015.

[10] Zhong ci Shi. The f-e-m-test for convergence of nonconforming finite elements. *Mathematics of Computation*, 49(180):391–405, 1987.

[11] L. Beirão da Veiga, F. Brezzi, A. Cangiani, G. Manzini, L. D. Marini, and A. Russo. Basic principles of virtual element methods. *Computer Methods in Applied Mechanics and Engineering*, 23:199–214, 2013.

[12] L. Beirão da Veiga, C. Lovadina, and D. Mora. A virtual element method for elastic and inelastic problems on polytope meshes. *Computer Methods in Applied Mechanics and Engineering*, 295:327–346, 2015.

[13] E. A. de Souza Neto, D. Perić, M. Dukto, and D. R. J. Owen. Design of simple low order finite elements for large strain analysis of nearly incompressible solids. *International Journal of Solids and Structures*, 33:3277–3296, 1996.

[14] C. R. Dohrmann and M. M. Rashid. Polynomial approximation of shape function gradients from element geometries. *International Journal for Numerical Methods in Engineering*, 53:945–958, 2002.

[15] Mohamed S. Ebeida and Scott A. Mitchell. Uniform random voronoi meshes. *Proceedings of the 20th International Meshing Roundtable*, pages 273–290, 2011.

[16] Mohamed Salah Ebeida. Vorocrust v. 1.0, Jul 2017.

[17] Carlos A. Felippa. *Introduction to Finite Element Methods*. University of Colorado, Boulder, 2004.

[18] D. P. Flanagan and T. Belytschko. A uniform strain hexahedron and quadrilateral with orthogonal hourglass control. *International Journal for Numerical Methods in Engineering*, 17:679–706, 1981.

[19] Michael S. Floater. Mean value coordinates. *Computer Aided Geometric Design*, 20:19–27, 2003.

[20] Arun Gain, Cameron Talischi, and Glaucio H. Paulino. On the virtual element method for three-dimensional elasticity problems on arbitrary polyhedral meshes. *Computer Methods in Applied Mechanics and Engineering*, 282, 11 2013.

[21] Xifeng Gao, Wenzel Jakob, Marco Tarini, and Daniele Panozzo. Robust hex-dominant mesh generation using field-guided polyhedral agglomeration. *ACM Transactions on Graphics*, 36, 2017.

[22] William J. Gordon and James A. Wixom. Pseudo-harmonic interpolation on convex domains. *SIAM Journal on Numerical Analysis*, 11(5):909–933, 1974.

[23] Thomas J. R. Hughes. *The Finite Element Method–Linear Static and Dynamic Finite Element Analysis*. Dover Publications, 2000.

[24] Pushkar Joshi, Mark Meyer, Tony DeRose, Brian Green, and Tom Sanocki. Harmonic coordinates for character articulation. *ACM Transactions on Graphics*, 26, 2007.

[25] Mika Juntunen and Rolf Stenberg. Nitsche's method for general boundary conditions. *Mechanics of Computation*, 78(267):1353–1374, 2009.

[26] Nam-Sua Lee and Klaus-Jürgen Bathe. Effects of element distortions on the performance of isoparametric elements. *International Journal for Numerical Methods in Engineering*, 36:3553–3576, 1993.

[27] Qiaoluan H. Li and Junping Wang. Weak galerkin finite element methods for parabolic equations. *Numerical Methods for Partial Differential Equations*, 29:2004–2024, 2013.

[28] Guang Lin, Jiangguo Liu, and Farrah Sadre-Marandi. A comparative study on the weak galerkin, discontinuous galerkin, and mixed finite element methods. *Journal of Computational and Applied Mathematics*, 273:346–362, 2015.

[29] Richard H. MacNeal. A theorem regarding the locking of tapered four-noded membrane elements. *International Journal for Numerical Methods in Engineering*, 24:1793–1799, 1987.

[30] Sebastian Martin, Peter Kaufmann, Mario Botsch, Martin Wicke, and Markus Gross. Polyhedral finite elements using harmonic basis functions. *Eurographics Symposium on Geometry Processing 2008*, 27(5), 2008.

[31] L. Mu, J. Wang, and Y. Wang. A computational study of the weak galerkin method for second-order elliptic equations. *Numerical Algorithms*, 63:753, 2013.

[32] L. Mu, J. Wang, and X. Ye. Weak galerkin finite element method for second-order elliptic problems on polytopal meshes. *International Journal of Numerical Analysis and Modeling*, 12:31–53, 2015.

[33] Lin Mu, Junping Wang, and Xiu Ye. A weak galerkin finite element method with polynomial reduction. *Journal of Computational and Applied Mathematics*, 285:45–58, 2015.

[34] Daniel Pantuso and Klaus-Jürgen Bathe. On the stability of mixed finite elements in large strain analysis of incompressible solids. *Finite Elements in Analysis and Design*, 28:83–104, 1997.

[35] M. M. Rashid. Incremental kinematics for finite element applications. *International Journal for Numerical Methods in Engineering*, 36:3937–3956, 1993.

[36] M. M. Rashid and P. M. Gullett. On a finite element method with variable element topology. *Computer Methods in Applied Mechanics and Engineering*, 190:1509–1527, 2000.

[37] M. M. Rashid and A. Sadri. The partitioned element method in computational solid mechanics. *Computer Methods in Applied Mechanics and Engineering*, 237–240:152–165, 2012.

[38] M. M. Rashid and M. Selimotić. A three-dimensional finite element method with arbitrary polyhedral elements. *International Journal for Numerical Methods in Engineering*, 67:226–252, 2006.

[39] J.-F. Remacle, J. Lambrechts, B. Seny, E. Marchandise, A. Johnen, and C. Geuzainet. Blossom-quad: a non-uniform quadrilateral mesh generator using a minimum cost perfect matching algorithm. *International Journal for Numerical Methods in Engineering*, 89:1102–1119, 2012.

[40] Béatrice Rivière. *Discontinuous Galerkin Methods for Solving Elliptic and Parabolic Equations: Theory and Implementation*. Society for Industrial and Applied Mathematics, 3600 Market Street, 6th Floor, Philadelphia, PA 19104-2688 USA, 2008.

[41] Mili Selimotić. *Polyhedral Finite-Element Approximants in 3D Solid Mechanics*. PhD thesis, University of California, Davis, 2008.

[42] J. C. Simo and F. Armero. Geometrically non-linear enhanced strain mixed methods and the method of incompatible modes. *International Journal for Numerical Methods in Engineering*, 33:1413–1449, 1992.

[43] J. C. Simo, F. Armero, and R. L. Taylor. Improved versions of assumed enhanced strain tri-linear elements for 3d finite deformation problems. *Computer Methods in Applied Mechanics and Engineering*, 110:359–386, 1993.

[44] J. C. Simo and M. S. Rifai. A class of mixed assumed strain methods and the method of incompatible modes. *International Journal for Numerical Methods in Engineering*, 29:1595–1638, 1990.

[45] Friedrich Stummel. The generalized patch test. *SIAM Journal on Numerical Analysis*, 16(3):449–471, 1979.

[46] N. Sukumar. Construction of polygonal interpolants: a maximum entropy approach. *International Journal for Numerical Methods in Engineering*, 61:2159–2181, 2004.

[47] Manil Suri. On the robustness of the h- and p-versions of the finite-element method. *Journal of Computational and Applied Mathematics*, 35:303–310, 1991.

[48] Theodore Sussman and Klaus-Jürgen Bathe. Spurious modes in geometrically nonlinear small displacement finite elements with incompatible modes. *Computers & Structures*, 140:14–22, 2014.

[49] Cameron Talischi and Glaucio H. Paulino. Addressing integration error for polygonal finite elements through polynomial projections: A patch test connection. *Mathematical Models and Methods in Applied Sciences*, 24:1701–1727, 2014.

[50] Cameron Talischi, Anderson Pereira, Ivan F. M. Menezes, and Glaucio H. Paulino. Gradient correction for polygonal and polyhedral finite elements. *International Journal for Numerical Methods in Engineering*, 102:728–747, 2015.

[51] Eugene L. Wachspress. *A Rational Finite Element Basis*. Academic Press, 1975.

[52] J. Wang and X. Ye. A weak galerkin finite element method for second-order elliptic problems. *Journal of Computational and Applied Mathematics*, 241:103–115, 2013.

[53] X. Wang, N.S. Malluwawadu, F. Gao, and T.C. McMillan. A modified weak galerkin finite element method. *Journal of Computational and Applied Mathematics*, 271:319–329, 2014.

[54] Robert Winkler. Comments on membrane locking. *Proceedings in Applied Mathematics and Mechanics*, 10:229–230, 2010.